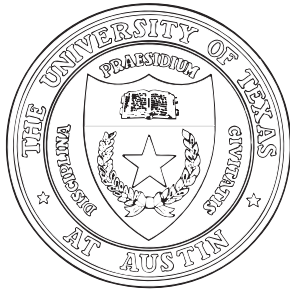


Scintillator wavelength-shifting fiber response to magnetic fields



Matthias Ihl, Christian Sämman,
Karol Lang

The University of Texas at Austin

9th June 2001

Abstract

In this report we investigate some magnetic properties of the scintillator and wavelength shifting (WLS) fiber used in the MINOS Detectors (Fermilab), namely the dependence of the light yield on magnetic fields. We give a detailed description of the experiment and also discuss the necessity of a magnetic field in the Calibration Module.

Contents

1	Introduction	3
2	Experimental Setup	4
2.1	Devices	4
2.1.1	Scintillator and wavelength-shifting fiber	4
2.1.2	Photomultiertubes (PMTs)	5
2.1.3	Magnetic coil	7
2.2	Layout of the setup/ description of the experiment	9
2.3	Data acquisition	10
2.3.1	QVT	10
2.3.2	NIM and CAMAC	11
2.3.3	Computer	11
3	Measurements	12
3.1	Gain of the middle PMT	12
3.2	The light-yield measurements	14
4	Conclusions	17
A	Cosmic Rays	18

1 Introduction

The goal of our project was to investigate the dependence of the light yield of the scintillators and wavelength-shifting fibers used in the MINOS (Main Injection Neutrino Oscillation Search) detectors on magnetic fields. Both the far and the near detector of MINOS consist of octagonal, toroidally magnetized, 1-inch thick steel planes, suspended vertically in large arrays. Each steel plane provides mechanical support for a plane of scintillator detector modules, which is attached to each steel plane.

Multi-turn coils are installed to produce a magnetic field of 1.5 T in the center of the plates (fig. 1).

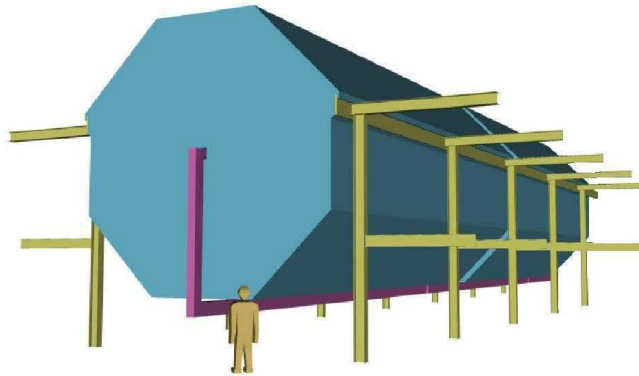


Figure 1: 3D model of the far detector with magnetic coil

There are two main purposes of the magnetic field:

- it is essential for momentum measurements of charged particles produced in an event
- to increase the acceptance of charged particles produced in an event

Even though the magnetic field in the center is quite high, it is concentrated in the steel plates, thus the expected magnetic field in the scintillators and WLS fibers is $\approx 0.04 \text{ T} = 400 \text{ Gauss}$.

Therefore we carried out experiments to investigate the influence of magnetic fields on the light yield of the scintillators/WLS fibers. Similiar experiments done at DESY indicate a small effect of about 1 percent at 400 Gauss.

Our experiments, as explained later, also show only a small dependence of the light yield on magnetic fields in the above named range of magnetic field strengths.

2 Experimental Setup

2.1 Devices

2.1.1 Scintillator and wavelength-shifting fiber

The scintillator used in MINOS is an extruded scintillator with a groove for a wavelength shifting fiber and a co-extruded TiO_2 coating as a reflector. The cross sectional profile (shown in fig.2) is 41 mm wide and 10 mm thick. The 2 mm deep groove in the upper surface accepts the 1.2 mm WLS fiber.

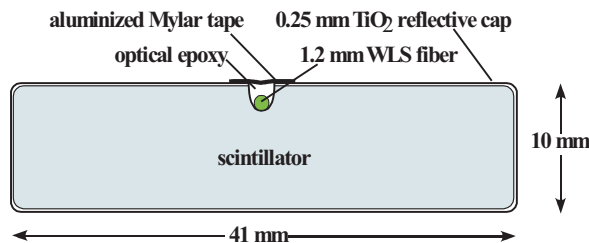


Figure 2: Cross-sectional profile of the scintillator

In our experiment we used a 0.9 mm WLS fiber. The scintillator is made from commercial grade Dow 663 polystyrene material. As primary dopant (1% per weight) for the polystyrene, PPO (2,5-diphenyloxazole) is used. The secondary dopant (0.03% by weight) is POPOP (1,4-bis(5-phenyloxazol-2-yl)benzene). The typical attenuation length of the scintillation light along the finished scintillator is 2 - 3 cm. In the scintillation process, blue photons are produced, which eventually hit the fiber, namely the WLS Y-11 fluor, where they are absorbed and re-emitted as green photons. The fibers are designed to give a maximum trapping fraction for green light. The inner core, containing the Y-11 fluors, is polystyrene (refractive index $n_1=1.42$), a thin intermediate layer is acrylic ($n_2=1.50$) and the thin outer cladding is polyfluor ($n_3=1.42$). The absorption spectrum of the Y-11 fluor (centered at 420 nm (blue)) has only a slight overlap with the emission spectrum, which is centered in the green beyond 470 nm. Thus, self-absorption in the fiber is very small. The attenuation length of the WLS fibers used for readout is 5-6m.

2.1.2 Photomultiertubes (PMTs)

For our setup, three PMTs were necessary: two were needed to determine coincidence events ("cosmic ray telescope" as described below) and one connected to the WLS fiber and scintillator, which we investigated. We will refer to the first mentioned as upper and lower "coincidence tubes" and to the third one as middle tube. The lower tube was a Philips 56AVP PMT, which we operated at 1789 V. The upper and middle tubes were Electron Tubes Limited 2" Photomultiplier Type 9954B, operated at 2017 V and 2000-2300 V, respectively. It was specifically important to know the characteristics of the middle PMT, which are summarized in table 1.

Table 1: Characteristics of PMT 9954B	
Window	
material	borosilicate glass
profile	plano-concave
diameter (max)	52.3 mm
index of refraction	1.48
Photocathode	
type	bialkali
active diameter	46 mm
spectral range	310-700 nm
corning blue (typ)	12.5
QE at peak wavelength (typ)	26%
Dynodes	
number	12
type	LF
secondary emitting surface	BeCu
capacitance anode to all dynodes	4pF
Gain and Dark Current	
voltage for 500 A/lm (typ)	1800 V
voltage for 500 A/lm (max)	2300 V
dark current at 500 A/lm (typ)	1.5 nA
dark current at 500 A/lm (max)	5 nA
dark count at 293 K (typ)	$800s^{-1}$
Magnetic Field Sensitivity	
The field for which the output decreases by 50 %	
field directed along dynodes	$1.2 \times 10^{-4}T$
field directed across dynodes	$2.0 \times 10^{-4}T$
field directed along axis	$6.0 \times 10^{-4}T$
Timing Performance	
rise time	2.0 ns
pulse width	3.0 ns
transit time	41 ns
transit time dispersion	1.9 ns
Temperature Coefficient	
(typ)	$\pm 0.3\%K^{-1}$

2.1.3 Magnetic coil

To produce fields similar to those expected in the scintillator planes of the two MINOS detectors, we first tried to design a setup using a Helmholtz coil. The advantage of this would have been a homogenous, strictly localized magnetic field, but after calculating, we found that the fields were too weak (with a reasonable amount of wire / current).

Since the homogeneity of the field is not important to determine, if there is an effect at all, we can do without a perfect homogenous field. A simple coil fitting our needs could be lent from Artur Widera (group of Dr. Raizen), who built it as a prototype for coils that will be used in a Zeeman slower.

The coil consists of a copper cylinder, bounded with two copper plates to fix the wire and to provide some cooling. There are 500 windings of copper wire (AWG 10, $\varnothing = 2.59 \text{ mm}$) on the coil covered with Thermaleze insulator. Its lifetime at 200° C is 20,000 h. The temperature of the coil can be measured by a thermo element fixed inside the coil.

The results of our measurements to obtain coil specifications as resistance etc. are shown in fig. 3.

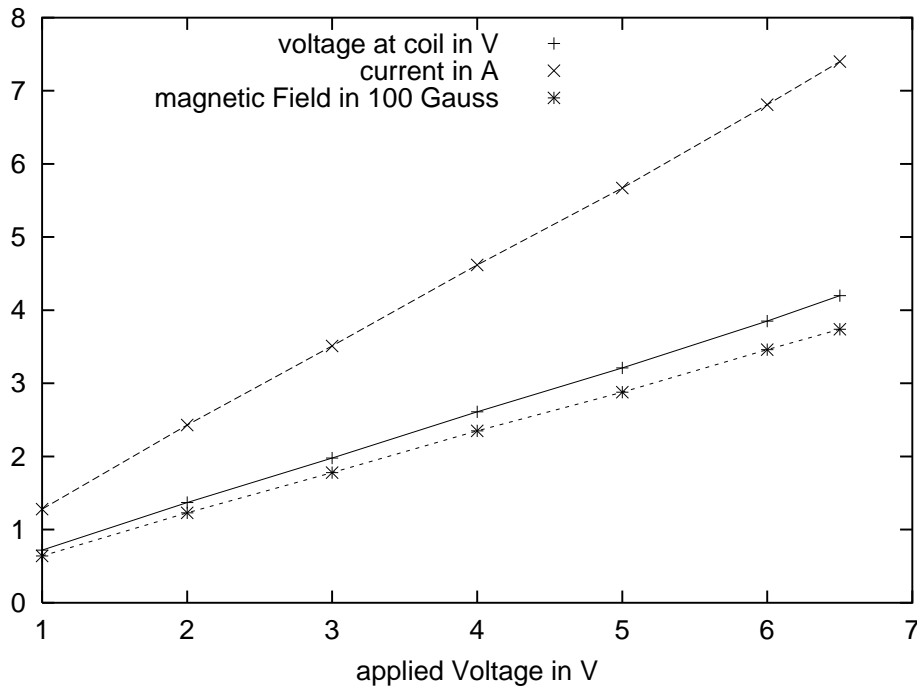


Figure 3: measurements of coil properties

With this data, we get the following results:

resistance/circuit	$0.874 \pm 0.006 \Omega$
resistance/coil	$0.5660 \pm 0.0005 \Omega$
power input/circuit (at 6 V)	40.86 W
power input/coil (at 6 V)	26.22 W

Thus we can easily achieve fields of about 380 Gauss. This should be enough to measure an effect on the light yield, if there is one at all. The field of the coil has a pseudo-gaussian shape (fig. 4).

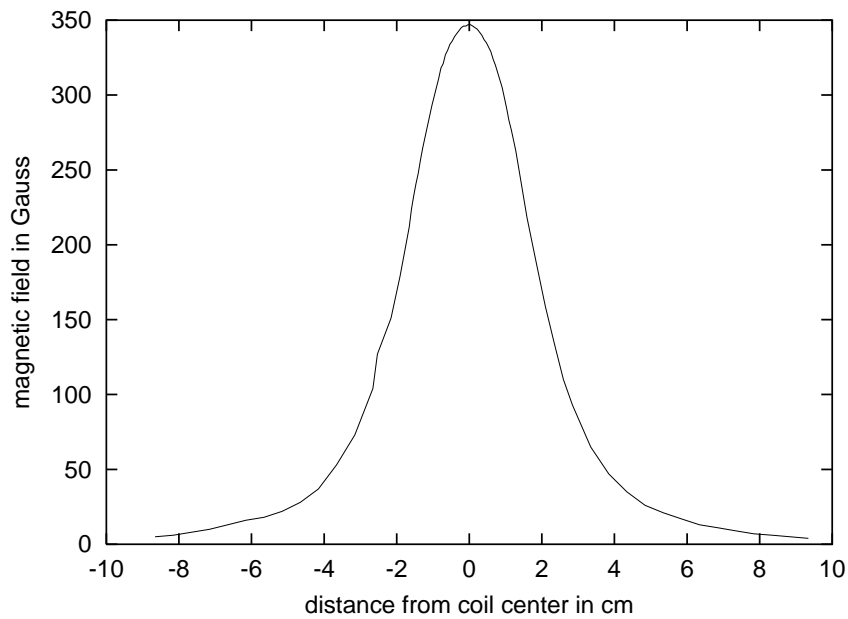


Figure 4: magnetic field of the coil at 6V

It is strictly localized and therefore doesn't affect the photomultiplier tubes. (The field near the tubes was measured to be below 0.5 Gauss before shielding.)

The temperature of the coil is in equilibrium below $50^\circ C$, and the difference of the temperature near the tubes is below $1^\circ C$.

2.2 Layout of the setup/ description of the experiment

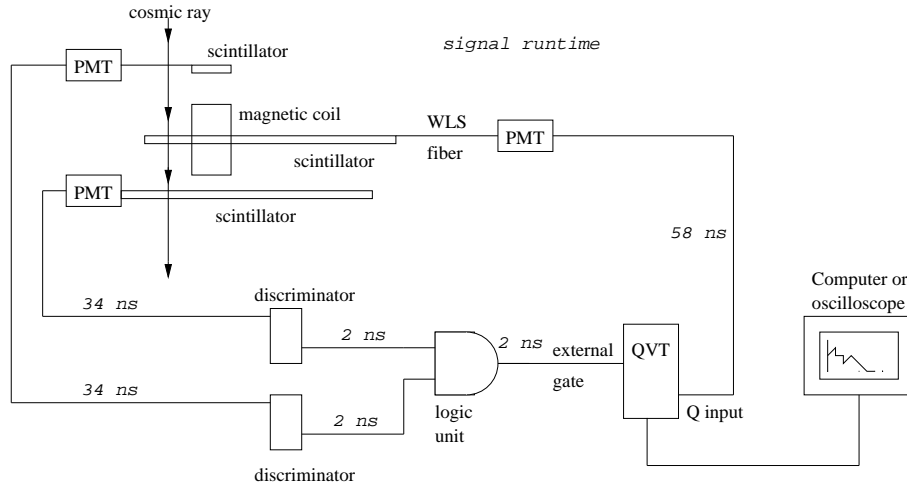


Figure 5: The experimental setup

As mentioned above, the goal of our experiment is to determine if there is a significant effect of a magnetic field on the light yield of the scintillator used in MINOS. A scintillator emits light when it is crossed by a high-energetic particle. Our options were to choose between cosmic rays (see app. A) and radioactive material as a source for these particles. Since the University of Texas requires a special safety training to be taken for handling radioactive material, we decided to use cosmic rays. The disadvantage of this method is the relatively long time to get a significant spectrum.

The layout of the experimental setup is schematically shown in fig. 5. It is basically a "cosmic ray telescope", a setup to measure the energy spectrum of high energetic particles, known as cosmic rays.

When cosmic rays cross scintillator material, they excite some of its molecules what results in a flash of photons. There is a fixed relation between the energy of the high energetic particle and the number of photons it produces. Thus, by measuring the photons, the particle's energy can easily be derived.

To measure the photons, the flash has to be conducted to a photomultiplier tube (PMT), which transforms each photon (or better each tenth, depending on the quantum efficiency of the PMT) into a fixed amount of electric charge, which can be read out by the QVT (see 2.3.1). The photons produced by a high-energetic particle (about 420 nm) bounce through the transparent scintillator, reflected by the TiO_2 coating. At some time, they will hit the wavelength-shifting fiber, fixed in a groove of the scintillator. There they are absorbed and

reemitted into the fiber, shifted in their wavelength to green (470 nm). The fiber now directly leads the photons to a PMT.

Our setup includes three of these cosmic ray detectors, each consisting of a scintillator strip, a wavelength-shifting fiber and a PMT. Two of them (the "upper" and "lower" ones) ensure that we really have a cosmic ray crossing our setup. If both detectors produce a signal at nearly the same time, it is very likely, that one particle crossing both scintillators, produced them. (In other setups, there are more than two coincidence detectors to decrease coincidence events by noise of the PMTs.) By crossing the scintillator strips orthogonally, a small area is selected for the detection of high-energetic particles, in which we can apply a magnetic field.

The signals from the upper and lower tubes are discriminated to logical pulses, so each time one of the PMTs detects a photon flash, a rectangular pulse of -0.6 V and 150 ns width is produced. If there is an overlap in the two pulses, another pulse of -0.6 V and 100 ns is generated by a logic unit and used to gate the QVT to read out the middle tube. Thus, each time a cosmic ray crosses all three scintillators (and therefore our well-defined area), the upper and lower tubes produce signals which generate a gate defining the time in which the QVT sums up the charge coming from the middle tube.

To be sure that the signal of the middle tube arrives at the QVT during the gating signal, non-zero signal runtimes in the wires and temporal delays between input and output pulse in the logical units had to be considered.

A magnetic field (see 2.1.3) up to 380 Gauss in the direction of the middle scintillator strip can be applied in the area defined by the orthogonally crossed upper and lower scintillators. Because of the sensitivity of the PMTs on a magnetic field, we had to make sure, that the magnetic field near the PMTs is far below one Gauss. At the nearest phototube (about 1 meter distance to the coil) we measured a field of 0.5 Gauss. Nevertheless, we shielded all PMTs with mu-metal.

Another problem was the heat generated by the coil. To prevent the scintillator strips from aging rapidly we wrapped it with aluminum foil, as well as the PMTs. Additionally, the temperature near the middle tube was measured before and after a spectrum was recorded. Thus, if a difference in the light yield is measured with magnetic field it is because of the field and not due to the heating or a residual field at the PMTs.

2.3 Data acquisition

2.3.1 QVT

We used the LeCroy Model 3001 QVT Multichannel Analyzer to analyze the data readout from the middle PMT connected to the WLS fiber and scintillator. The QVT can histogram

any one of three parameters: charge (area), voltage (peak) and time (start/stop). For our experiment we used the Q mode, which has a sensitivity of 0.25 pC/channel. The input current is integrated for a duration ranging from 20 ns to 1 μ s. Each of the 1024 channels has a count capacity of 16 bits. The contents may be displayed in linear or logarithmic fashion on any X-Y oscilloscope or a computer. Using all four 256-channel quadrants results in a total charge range of 0 - 256 pC \pm 10%. We operated the QVT via an externally applied gate pulse (EXT GATE), which was generated by coincidence events as described above.

2.3.2 NIM and CAMAC

NIM (National Instrumentation Methods) is a standard modular instrumentation system, consisting of standard modules, the bins in which they are housed and associated power supplies. NIM instrumentation for this experiment included:

1	Phillips Scientific Model 711 six channel discriminator
2	Phillips Scientific Model 756 quad four-fold logic unit
3	LeCroy Model 3001 qvt multichannel analyzer

Unfortunately, there is no possibility to connect NIM modules directly to a computer, so we had to make use of the CAMAC (Computer Automated Measurement And Control) instrumentation system in addition to the NIM, in order to establish a connection between the QVT and a computer. For this purpose we used: (including other CAMAC instrumentation)

1	LeCroy Model 2301 qvt - CAMAC
2	LeCroy Model 8901A GPIB Interface (to computer)
3	CAEN Model C243 8 Channel 100 MHz Scaler

2.3.3 Computer

As mentioned above, the data was readout to a computer. An existing C program named "qvt001.c" was modified for our specific purposes. Its main task was to establish a connection to the GPIB interface and transfer the data to the computer, where it was stored in a file. We used "GNUplot" to plot and evaluate the data, i.e. fitting the data. This method was used to determine the gain of the middle PMT(see Chapter 3: Measurements).

3 Measurements

3.1 Gain of the middle PMT

The first property we measured was the gain of the middle PMT, in order to be able to calculate the number of primary electrons and finally the rough number of photons arriving in the tube per event.

The gain can be easily obtained by measuring the one-photoelectron-amplification. An energy spectrum is recorded by running the setup with a fast internal gate of the QVT, a simple rectangular wave. (The exact properties of the signal, like width and amplitude, don't matter in this case.) The distribution looks typically like fig. 6. For small QVT-channels, there are nearly no counts. Then at a certain channel (in fig. 6 at 65) a sharp pedestal is found. This pedestal represents the charge the QVT received by recording the noise of the PMT during the gate interval, so it can be regarded as the zero-point for the further calculation. (In the shown plots, the pedestal is often cut off by scaling.) Next to this sharp

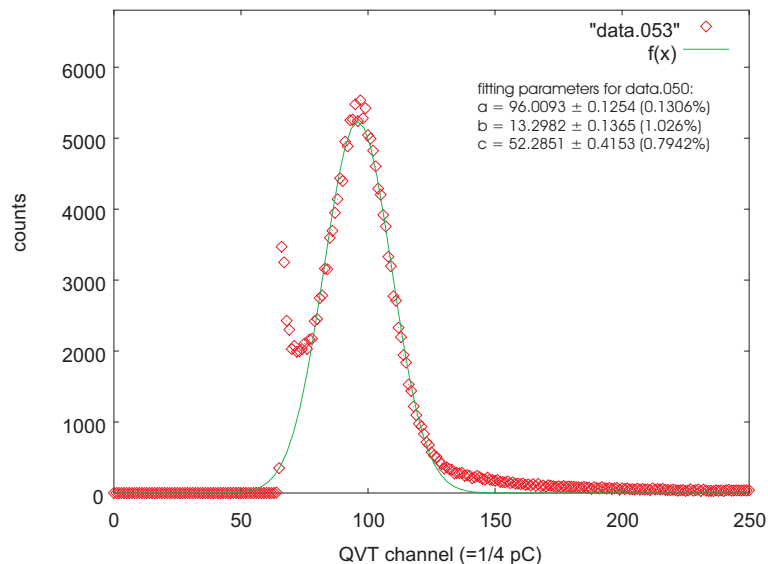


Figure 6: The one-electron-amplification of the middle tube at 2300V

peak, there is a gaussian distribution, resulting from single photons which reach the PMT despite the box covering the setup. (At first, we applied a diode as a weak light source in the box, but we realized, that this was not necessary.)

These single photons produce single primary electrons in the PMT, which are the main contribution to the gaussian distribution. (The contribution of two or more electrons can be

neglected, but they explain the deviation of the experimental data to the gaussian fit at the right edge.)

The gain is now obtained by fitting a gaussian distribution to a sensible chosen interval in the spectrum, subtracting the position of the pedestal from the position of the maximum of the gaussian distribution and deviding the corresponding charge by the elementary charge. The gaussian function used is:

$$f(x) = 100c \cdot \exp\left(-\frac{(x-a)^2}{2b^2}\right) \quad (1)$$

with a the maximum and b the standard deviation usually denoted by σ . The 100c makes sure, that the adjustments of the fitting parameters are in the same order of magnitude.

With the fitting parameters in fig.6, we get the following results:

QVT channel of pedestal	65
fitting interval (channels)	[75; 200]
QVT channel of maximum	96
charge correspondent to difference	7.75 pC
gain of PMT	$48.4 \cdot 10^6$

Amplification ratios of the magnitude 10^6 are common.

Unfortunately, the PMT turned out to be very noisy at this voltage, so we had to decrease it. This resulted in a not so clearly expressed gaussian as in the first case (see fig. 7).

QVT channel of pedestal	65
fitting interval (channels)	[70; 200]
QVT channel of maximum	74
charge correspondent to difference	2.25 pC
gain of PMT	$14.0 \cdot 10^6$

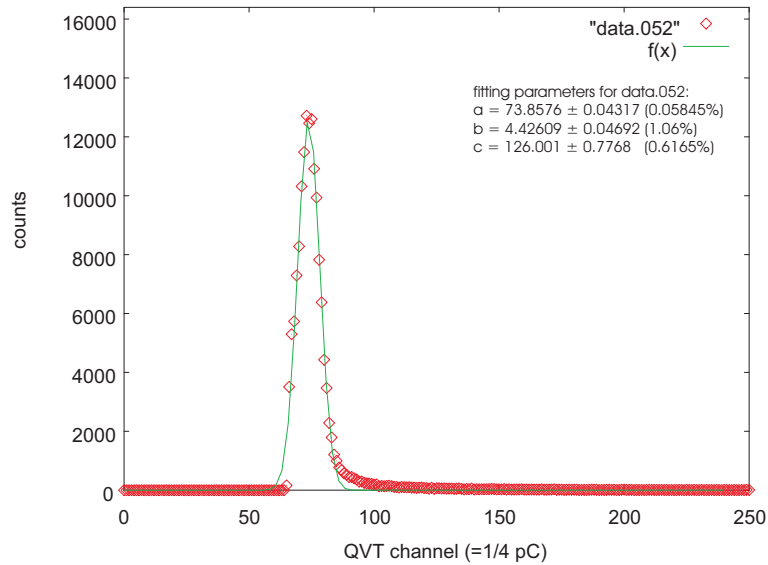


Figure 7: The one-electron-amplification of the middle tube at 2017V

3.2 The light-yield measurements

After making sure that the middle tube operates with a reasonable gain, we went on to record the energy spectrum with and without magnetic field. Since we are only interested in the difference of the two spectra, no calibration work had to be done (except for the signal runtimes and the logical pulses' widths).

Because the coincidence area that can be crossed by cosmic rays is rather small, it takes a long time to record a spectrum (the both shown took 5 days each). Together with difficulties with the calibration and the very noisy signals of the PMTs available, we were not able to obtain a lot of data. The only two sensible spectra are shown here, and it is obvious, that the value of their analysis is limited.

The spectra (fig. 8 and 9) basically look like a broadened one-electron-spectrum. Nearly no counts up to a certain channel, where a pedestal is found, followed by the energy distribution of the high energetic particles crossing our setup.

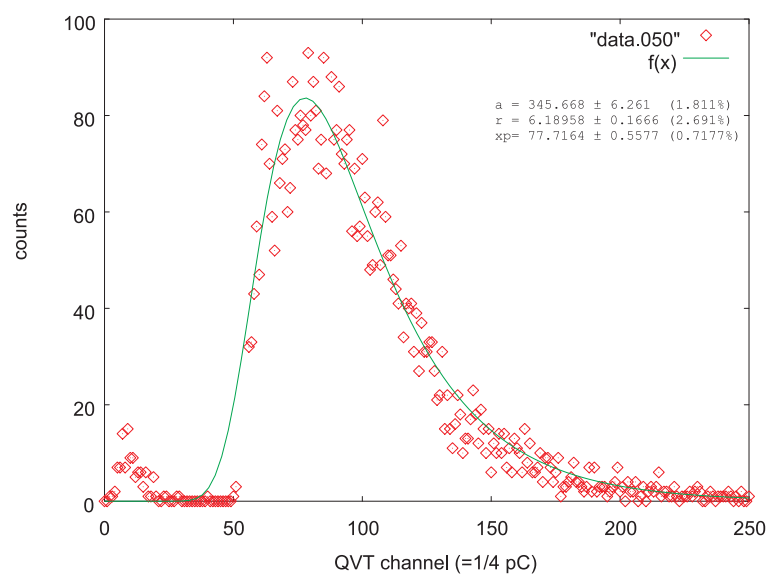


Figure 8: Cosmic ray spectrum without magnetic field

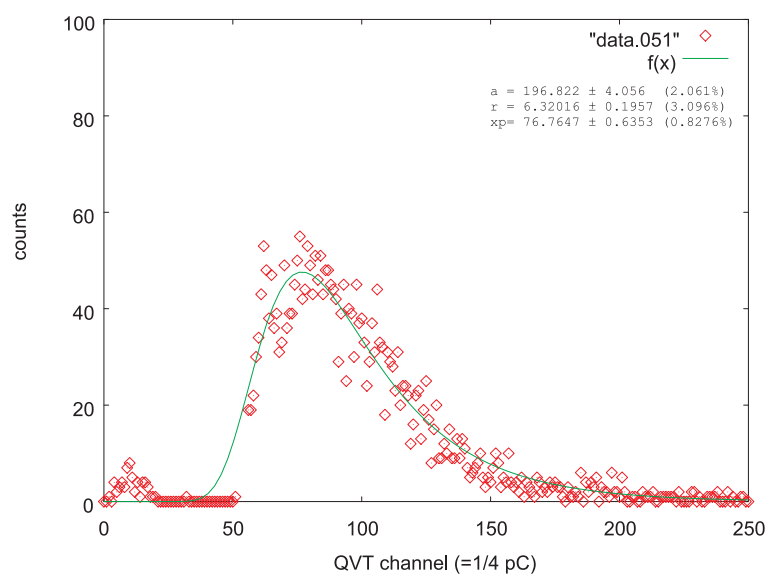


Figure 9: Cosmic ray spectrum with magnetic field

In our spectra, there are small peaks left of the pedestal. Since integrating over the PMT noise should at least lead to a count in the pedestal channel, this is not physical. We tried to get rid of them by increasing the signal runtime of the middle PMT and adjusting the gate widths with some success, but to eliminate the peak completely we would have had to decrease our gate width below a reasonable value. (Note that the gate width is smaller than the internal one of the QVT as the pedestal is shifted to the left.) The pedestal itself is located at channel 53 in both cases, it is cut off again due to scaling of the plot. We used the Landau distribution to fit the data:

$$f(x) = a \cdot \frac{\exp(\frac{1}{2}(\frac{r}{100}(x_p - x) - \exp(\frac{r}{100}(x_p - x))))}{\sqrt{2\pi}} \quad (2)$$

where x_p is the maximum of the distribution. The fitting results are listed below:

	without magnetic field	with magnetic field of 350 Gauss
a	345.668 ± 6.261 (error: 1.811%)	196.822 ± 4.056 (error: 2.061%)
r	6.18958 ± 0.1666 (error: 2.691%)	6.32016 ± 0.1957 (error: 3.096%)
x_p	77.7164 ± 0.5577 (error: 0.7177%)	76.7647 ± 0.6353 (error: 0.8276%)

The fits suggest a higher light yield without magnetic field, which is not the sensible. Regarding the error of the fitting parameters, it is obvious, that the measured maxima do not contradict each other. Since the effect is expected to be of the order of 1%, it is clear, that our setup can not be used to measure this effect (at least not with the current calibration and middle PMT). The only statement we can make without doubt is that the effect with the magnetic field (350 Gauss) is not bigger than 5%.

4 Conclusions

The results of the measurements described in the last chapter are obviously not sufficient to determine if there is any effect of the magnetic field on the light yield of the scintillators and WLS fibers used in MINOS. However, it was possible to establish an upper limit for the maximum dependence on magnetic fields.

The possible effect should not be bigger than 5%. Experiments previously carried out at DESY ([2],[3],[4]) indicate that the influence of magnetic fields on plastic scintillators comparable to ours is about 1 % in the range of 350 - 400 Gauss.

From our point of view it is therefore not necessary to include a magnetic field in the Calibration Module (CM) for the MINOS detectors. The effect on the light yield is clearly too small to justify the costs of installing a magnetic coil in the CM.

After all, we have no experimental evidence that could support such an intent.

There are several proposals we can make for future experiments:

- use of radioactive material instead of cosmic rays to get higher count rates and reduce time of measurement
- new consideration of the signal runtimes
- recalibration of the logical pulses
- use of better, i.e. less noisy, PMT

Appendix

A Cosmic Rays

Cosmic rays were first discovered in 1912 as the cause for leakage in electrometers. Since they entered very fast the popular press, there is no strict scientific definition of cosmic rays. Popular speaking, they are "things that rain down from the heaven and are not wet".

Cosmic rays at sea-level are generated by primary particles hitting the earth's outer atmosphere, generating cascades of secondary particles.

The sources for these primary particles are high energetic solar particles as well as galactic cosmic rays. The last ones hit the earth 100,000 times per squaremeter and second. They consist mainly of protons (92%) and α -particles (6%). In the atmosphere, the primary par-

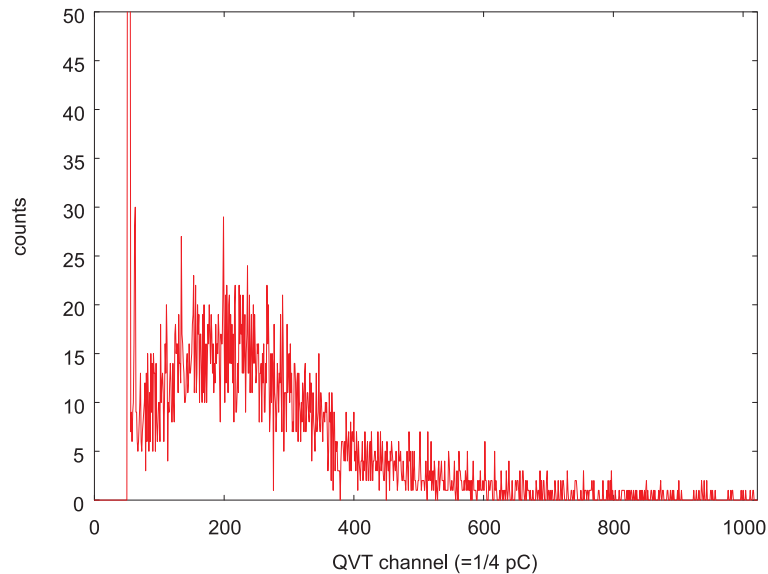


Figure 10: Cosmic ray spectrum

ticles interact with the nuclei of the atmospheric gases (N_2 , O_2) via nuclear force. A typical decay cascade is that of a proton into three pions, each pion decaying into a muon and a muon-neutrino and each muon into an electron, an electron-neutrino and a muon-neutrino:

$$p \rightarrow \pi + \pi + \pi \quad (3)$$

$$\pi \rightarrow \mu + \nu_\mu \quad (4)$$

$$\mu \rightarrow e^- + \nu_\mu + \nu_{e^-} \quad (5)$$

(Since this is a primary decay channel, the ratio of electron-neutrinos to muon-neutrinos at sea-level should be 1:2, experimentally determined was 0.64 ± 0.05 . The missing muon-neutrinos could be easily explained, if there was an oscillation of the neutrinos.)

The cosmic ray sea-level flux depends on the location on the earth (as the earth's magnetic field, which depends on the observers location, provides a shield against cosmic rays), the daytime and the solar activity (as many of the particles come from the sun).

In our experiment, we assumed the energy distribution of the cosmic ray particles to be constant during the time of measurement.

Fig. 10 shows a typical cosmic ray energy spectrum, recorded with our first setup. Since the area in which cosmic rays can be detected was not reduced to that of the magnetic field as in our final setup, the spectrum is much better than that shown in section 3.

References

- [1] Peter Litchfield
Does the Calibration Module need a Magnetic Field ?
NuMI-L-xxx, August 2000
- [2] T. Kamon *et al.*
A new scintillator and wavelength shifter
Nuclear Instruments and Methods 213 (1983) 261-269
- [3] D. Blömker *et al.*
Plastic scintillators in magnetic fields
Nuclear Instruments and Methods A311 (1992) 505-511
- [4] J. Mainusch *et al.*
Influence of magnetic fields on the response of a uranium scintillator electromagnetic calorimeter
Nuclear Instruments and Methods A311 (1992) 505-511
- [5] P. Adamson *et al.*
MINOS Technical Design Report
NuMI-L-337, October 1998
- [6] PHILIPS Data Handbook
Electron Tubes
Book T9, 1987
- [7] Donald E. Knuth
The T_EXbook
Addison Wesley Publishing Company, 1989
- [8] D. F. Anderson *et al.*
Development of a Low-Cost Extruded Scintillator with Co-Extruded Reflector for the MINOS experiment
FERMILAB-Conf-00/261-E